

ZIPNN: LOSSLESS COMPRESSION FOR AI MODELS

Moshik Hershcovitch^{1,2} Andrew Wood³ Leshem Choshen^{1,4} Guy Girmionsky¹ Roy Leibovitz⁵
 Ilias Ennmouri¹ Michal Malka¹ Peter Chin⁵ Swaminathan Sundararaman¹ Danny Harnik¹

ABSTRACT

With the growth of model sizes and the scale of their deployment, their sheer size burdens the infrastructure requiring more network and more storage to accommodate these. While there is a vast model compression literature deleting parts of the model weights for faster inference, we investigate a more traditional type of compression – one that represents the model in a compact form and is coupled with a decompression algorithm that returns it to its original form and size – namely lossless compression.

We present *ZipNN* a lossless compression tailored to neural networks. Somewhat surprisingly, we show that specific lossless compression can gain significant network and storage reduction on popular models, often saving 33% and at times reducing over 50% of the model size. We investigate the source of model compressibility and introduce specialized compression variants tailored for models that further increase the effectiveness of compression. On popular models (e.g. Llama 3) *ZipNN* shows space savings that are over 17% better than vanilla compression while also improving compression and decompression speeds by 62%. We estimate that these methods could save over an ExaByte per month of network traffic downloaded from a large model hub like Hugging Face.

1 INTRODUCTION

With scale, we have learned that models gain stronger abilities and with it, gain popularity. With scale, models also require more storage space and memory and with popularity more communication bandwidth. Taken together, we observe strains on communication bottlenecks that call for efficient solutions. Storage requirements, while often ignored, may accumulate to hundreds or thousands of times the size of a model if checkpoints (Biderman et al., 2023) or distributed updates are to be saved (c.f., 6) (Kandpal et al., 2023; Don-Yehiya et al., 2023; Zhang et al., 2021).

Similarly, models are repeatedly moved around in multiple channels: from a storage hub to inference machines; from training/fine-tuning nodes to the storage backend; between GPU nodes during distributed training, and so on. Network hubs epitomize the strains by model size. For instance, with over 14.5 GBs and 2.77 M downloads per month from Hugging Face (Wolf et al., 2019) Mistral (Jiang et al., 2023) alone requires 40 PBs of transferred information a month.

A large body of work has been aimed at reducing model sizes focusing on the parameter sizes and the number of computations in inference. Such methods transform the model

into a smaller one in an irreversible fashion. For example, distillation (Gou et al., 2021), pruning (Ma et al., 2021) and quantization (Gholami et al., 2021) all lose some information and, potentially, performance, for improved efficiency. Since these methods’ main focus is on inference speed, they are bound to the format of an actual running model. As such, they don’t necessarily push the space-saving to its limits, and are not stored in the minimal possible way.

In this work, on the other hand, we follow a more traditional definition of compression typically used for networking and storage. Compression that is also accompanied by a decompression process, returning a model to its origin – namely lossless compression.

Surprisingly, we observe (§3) that even standard lossless compressors like zlib (Deutsch & Gailly, 1996) or zstd (Collet & Kucherawy, 2018) can achieve non-negligible savings. While common rationale expects model parameters to have high entropy and therefore be non-compressible, we find that in reality there is less entropy than what the representation offers. Our goal is therefore to find a compression method that maximizes compression benefits for models while also being aware of compression and decompression speeds.

We identify the source of model compressibility as the floating point range that actually exists in models. Specifically, we find that the exponent component in a floating point parameter is highly skewed and therefore very compressible.

¹IBM Research ²Tel Aviv University ³Boston University ⁴MIT
⁵Dartmouth College. Correspondence to: Moshik Hershcovitch <moshik1@gmail.com>.

To this end, we devise a compression method that separates the exponent bits from the rest of the bits that often show no compressibility. We also identified that the source of compressibility of the exponent is entirely the skewed distribution of single bytes. This means that compressors that search for multi-byte repetitions are both unnecessarily time-consuming and unhelpful in this case, and in particular all of the Lempel-Ziv algorithms (Ziv & Lempel, 1977; 1978) hardly achieve any data reduction. Instead, we use only *Entropy Encoding* and specifically Huffman codes (Huffman, 1952), improving both performance and compression ratio in doing so. Another speed improvement comes from identifying the non-compressible parts and avoiding time-consuming compression attempts on them. The observations described above are relevant to most of the models, but not all of them. *ZipNN* therefore identifies the characteristics of the model at hand and determines which strategy best suits it.

The compression benefits are typically tied directly to the model parameter type. The BF16 model family is best compressed, as the exponent in BF16 accounts for half of the total bits (8 of the 16 bits), such models gain approximately 33% of space savings - reducing the exponent by $2/3$ amounts to reducing the full model size by $1/3$. In contrast, typical FP32 models show space saving of just 17% as the exponent accounts for $1/4$ of the model parameters.

We classify popular models into categories with distinct compressibility traits. We highlight the *clean models* category, where models have undergone some rounding after the training phase. The rounding allows compression of the other bits (apart for the exponent) and therefore clean models achieve effective compression, at times reaching 55% savings. For example, the popular RoBERTa model (Liu et al., 2019b) falls into this category. Our compressor is therefore challenged with the task of inline identifying the potential space savings in such a model and compressing it accordingly.

When comparing *ZipNN* to a state-of-the art compressor like Zstd we get the following improvements: On BF16 models our compressor achieves a 17% improvement in compression ratio and a 62% speedup in compression/decompression. For clean models, this is even larger with a 34% improvement in space and a 4.6X speedup in compression time and 83% speedup in decompression.

Finally, we explore the benefits of delta compression and show that by compressing the delta between two similar models one can achieve compression far greater than compressing a standalone model. This is useful for checkpointing and management of model variations.

The main contributions of this paper can be summarized as:

- We observe that lossless compressors may be effective

Table 1. Top ranked downloaded models from Hugging Face.

Model name	Model Size	#Monthly Downloads	Rank	Compressed Size
Bge	0.4 GB	434M	#1	42.1%
Mpnet	0.4 GB	226M	#2	82.9%
Bert	0.4 GB	85M	#3	83.9%
Qwen	3.1 GB	50M	#6	66.9%
Whisper	6.2 GB	40M	#7	42.7%
xlm-RoBERTa	2.2 GB	39M	#8	42.3%
Clip	0.6 GB	28M	#10	49.7%
Llama 3.1	812 GB	14M	#20	67.2%

for AI models and identify the source of their compressibility.

- We introduce a **new lossless compression method** tailored for AI models, which achieves a **better compression ratio** and **faster** compression and decompression.
- We categorize models according to their compressibility, highlighting that on the popular BF16 models, *ZipNN* can **reduce the model size by 33%**, and on so-called clean models by over a half.
- We study the potential of delta compression for checkpointing and model versions, learning that although during training all model weights constantly change, fewer bits are changing in every epoch, leading to better delta compression.

2 BACKGROUND

2.1 Motivation - use cases

With small models weighing about a Gigabyte (Devlin et al., 2019) and large ones Terrabytes (Fedus et al., 2021) storage and network overheads become an issue for many purposes. Moreover, common use cases require many model types or model versions and hence increased resources. We list some below as a motivation.

2.1.1 Model Hubs

Large model repositories or hubs like Hugging Face (Wolf et al., 2019), Model Zoo (Yu Koh, 2018), PyTorch (Pytorch, 2019), Tensorflow (Google, 2018), Adapter (Pfeiffer et al., 2020), IBM watsonx.data (watsonx.data) and Qualcomm® AI (Qualcomm AI Hub) hold a large number of models and serve numerous download requests of popular models. Hugging Face, the largest of these hubs, revealed in a statement in August 2024, that it holds 1.3M models, with a cumulative storage space of 12PB. They also serve 1 billion daily requests amounting to a network bandwidth of around 6 PetaBytes per day! Table 1 shows some of the

top-ranked models¹ and their compression ratio (using the methods described in Section 2.3). As seen, the potential traffic savings from compression is substantial.

In this use case, there are three ways in which compression can be beneficial, the first and the most important is to reduce the amount of data transferred, the second is to reduce the amount of data stored and the third is to reduce the time to download and upload those models.

2.1.2 Distributed and Decentralized Training

During training of large models, training nodes transfer data between them to overcome the need to save the full model and computation on a single GPU/node. In some methods, only the model weights are transferred between nodes, and in other methods, the optimizer weights and gradients are transferred as well (Zhao et al., 2023). Either way, distributed training is usually limited by data transfer between nodes, an issue compression addresses directly. For example: FSDP (Fully Sharded Data Parallel) is a PyTorch method that during training, in addition to transferring model weights, also transfers gradients and optimizer states, causing a networking bottleneck that limits the training of large models.

Another training paradigm is decentralized or federated training, which proposes accommodating training of the same model by different contributors. This ranges from federated learning that contributes gradients (Zhang et al., 2021), to contributing partially trained models (Li et al., 2022), from changing the kinds of updates done (Lialin et al., 2023) to relying on volunteer computing (Diskin et al., 2021), or even relying on different objectives and expertise all merged into the same model (Don-Yehiya et al., 2023). All of these methods inherently transfer and store numerous model versions, which also drove dedicated version control frameworks (Kandpal et al., 2023).

2.1.3 Checkpoints and Versions

During model creation, multiple intermediate versions of the models are commonly saved. This often includes tests on the training regime such as hyperparameter tuning (Turner et al., 2021). Even during the training of a single model, the current model is periodically checkpointed to recover after a crash, to select the best checkpoint from a few options (Dodge et al., 2020), for analysis (Biderman et al., 2023), improve performance (Junczys-Dowmunt et al., 2018; Sandler et al., 2023), etc. Even though saving during checkpointing rarely slows the training time, it does burden the networking and storage, limiting the frequency and amount of saved and shared checkpoints, which are encouraged by the community (e.g.; (Biderman et al., 2023; Liu et al., 2023)).

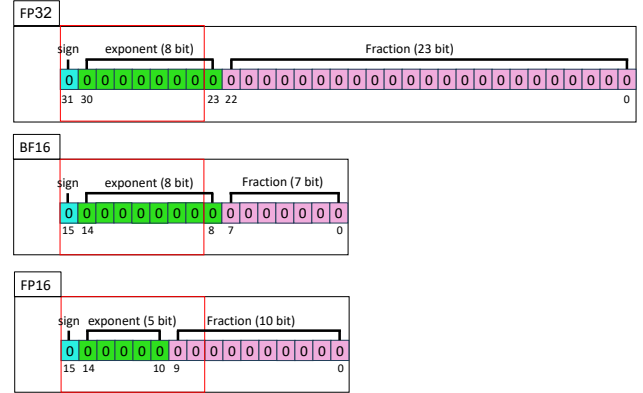


Figure 1. Representation of FP32, BF16, FP16 floating point types.

2.2 Models Structure and Types

Regardless of the architecture, current models are mainly composed of matrices or tensors of different sizes and a code that can read the parameters in the matrix and convert it to a function. While a layer may contain several such tensors, for brevity we call each tensor a layer. We note that the code is negligible in weight and hence the main focus of our compression is reduced to tensors, or even put more simply, long arrays of numeric parameters.

The type of those numbers is a key factor in the ability to compress the model parameters. Parameters typically represent real numbers and as such the most straightforward standard approach is to represent them with *floating point* numbers. The floating point format represents a flexible scale with a fixed number of bits which allows for larger numerical ranges. In a nutshell, floating point contains an exponent part - indicating the range in which the real number lies, a *mantissa* or *fraction* pointing to the actual number within this range, and a sign bit denoting whether a number is positive. For example, FP32 is a 32 bit floating point number with a sign bit, an 8 bit exponent and a 23 bit mantissa (see Figure 1). The real number is calculated by $(-1)^{\text{sign}} \cdot 2^{\text{exponent}-127} \cdot 1.\text{fraction}$. Many models are trained with FP32 for its high precision or a mix of precisions. Later during inference, the models sometimes keep their original format, but often choose to forgo some precision for a more compact representation and more efficient computation (Shoeybi et al., 2019; Granite Team, 2024; Dubey et al., 2024). Perhaps the most popular parameter type used for inference models is BF16 (Wang & Kanwar, 2019) which cuts the tail end of the fraction (hence reducing the precision level) but maintains the same exponent as shown in Figure 1. Other options include FP16, or quantized models using integer parameters with fixed precision.

¹Rank as of October 2024.

2.3 Lossless compression

Lossless compressors are the traditional form of compression and are widely used for reducing network and storage overheads in all fields of computing. They consist of two algorithms – compression and decompression, where after applying both in sequence the output returns to the exact same state. There are countless compression techniques and they vary in the tradeoff between compressibility and compression/decompression time (see for example (Squash, 2016)).

Throughout the paper, we measure the effectiveness of compression using *compression size* in percent. Namely, the percentage of the data that is left after compression – *lower is better*. For example, if the method compresses a GB into a quarter of a GB it has a compressed size of 25%.

The main techniques employed in lossless compression are based on repetition removal (stemming from the seminal works of Lempel and Ziv (Ziv & Lempel, 1977; 1978) and dubbed LZ compression) and entropy encoding (e.g. (Huffman, 1952; Rissanen, 1976)). LZ compressors find multiple-byte repetitions (typically of at least 4 bytes) and replace these with shorter back-pointers, hence saving space. Entropy encoding, on the other hand, looks at the entropy seen in the distribution of single bytes and reduces the length by working at a bit-level granularity, coding popular bytes with short representations. The most popular compressors combine the two techniques (first repetition removal and then entropy encoding), for example Zlib (Adler & Gailly, 2024) and Zstd (Collet, 2024b).² A second family of compressors, that favors speed over compression ratio, relies solely on LZ repetition removal, e.g. LZ4 or Snappy (Collet, 2024a; Dean et al., 2024).

3 COMPRESSION FOR MODELS

In this section, we introduce *ZipNN* – our variants of lossless compression specifically tailored for model compression. We will first discuss compression of the majority of models and model contents. As mentioned in the introduction, we classify models into two categories - regular models and what we call *clean* models. Clean models are models that have undergone various techniques like number rounding or transformation between parameter types. These transformations typically leave many bits as zeros and increase model compressibility. However, once such a model is re-trained or fine tuned, it quickly becomes less compressible and behaves like a regular model. Regular models form the majority of models, and are models that were trained and remained unmodified after the training phase. In addition,

²In our experiments, we chose Zstd as the underlying compressor/decompressor due to its superior speed vs. compression tradeoff (Collet, 2024b; Squash, 2016).

we note that model formats also contain some metadata and at times a few layers that behave differently (for example tensors of parameters that contain integers). These typically constitute a negligible part of the model and hardly affect the model compression ratio. Later in the section, we will discuss clean models and variations.

3.1 Regular Model Compressibility

Simply deploying standard compressors to a model produces mixed results. For most models, using an LZ-type compressor like LZ4 or Snappy yields no gains at all. This is expected since it requires the data to contain sequences of bytes that repeat. However, model tensors are both noisy and unstructured - meaning that parameters typically do not have an affinity with their neighbors. This makes repetitions that span multiple parameters scarce.

Using a compressor that also combines entropy coding, such as Zlib or Zstd, does show some compressibility. Initially, one may expect models to be non-compressible and show high entropy, as parameters may encode unpredictable information and differ from each other. This is correct to a certain degree, but in reality, the actual range in which parameters reside is typically limited, which reduces the entropy and opens the door for compression to be effective.

A deeper dive shows that models indeed contain a high level of randomness in their parameters, but this is true for the fraction and sign bit parts of the floating point parameter. The exponent on the other hand is highly skewed and is the source of the compressibility. Figure 2 shows the distribution of the exponent in four different models. This distribution is highly skewed, and strikingly similar between different models, whether BF16 or FP32. It is very similar among language models but also close when testing other model types, such as Resnet which is an image model. Out of the 256 possible values in the exponent, we see only around 40 that actually appear (50 in the image model). Moreover, the top 12 values account for almost 99.9% of all parameters (17 in the image model).

This highly skewed distribution can be explained as an artifact of the way models are trained. Model weights are initially set in the space of [-1,+1] and the training process scarcely pushes weights out of this range, perhaps since weights can have sufficient impact without the need to grow substantially. This explains why exponent values do not tend to exceed 128 which translates to the range [-1,1]. On the other hand, we see that weights are also not found in the lower ranges of extremely high precision. This is likely a result of various choices in the training process, for instance, optimizers (e.g. the Adam optimizer) add some noise in order to avoid division by zero. This noise is set in the order of 2^{-23} (corresponding to an exponent of around 99), and thus weights do not fall much below this noise level.

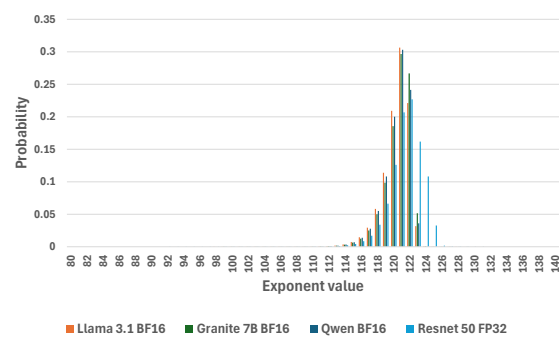


Figure 2. Histogram of exponent values for four different models. The graph is focused only on middle values and no exponent values appear outside this range. Based on 1GB taken from the middle of the model.

Exponent Extraction. No matter the reason that the exponent is skewed, we leverage this skewed distribution for tailoring our compression method. It is clear that mixing exponent data with either the sign bit or the fraction bits will interfere with the compression of the exponent. We therefore choose to rearrange the data in a way that separates the exponent data. We call this *exponent extraction* and it is depicted in Figure 3 for a BF16 based model.

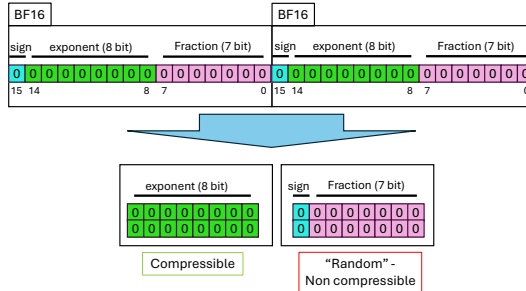


Figure 3. Exponent Extraction for BF16 - group all exponents into a separate compression stream.

Huffman only Compression. In addition, we observe that there is no structure in the tensors, namely that the exponents are not ordered in any way. Whatever repetitions are found by an LZ type compression, these are most likely “random” in the sense that they are an artifact of the skewed distribution. We therefore forgo the LZ compression part and use only an entropy encoder and specifically we use Huffman encoding. This proved to be helpful both in terms of compression/decompression performance, which is expected, but also in improving the compression ratio. It turns

out that the random repetitions found by the LZ phase are naturally short, and not only do they not save much, but they also interfere with the effectiveness of the Huffman encoder (by adding back-pointers to the mix). In order to ensure that the repetitions found are indeed “random”, we ran a test by which we do a random shuffle of the parameters in a model and then compress the exponents using Zstd. The shuffled version reached nearly the same compression ratio (up to 0.05%). Our experiments show that using Huffman encoding gives a very good trade-off of time vs. space. An FSE entropy encoder achieves a slightly better compression ratio (0-2%) at the expense of significant performance penalty (at times over 2X).

Figure 4 shows the compression ratio benefits of each of the steps that we use. We see that using Huffman without exponent extraction is only helpful for speed over Zstd. However, once we divide the exponent from the rest of the data, using Huffman vs Zstd also achieves better compression (as well as speed).

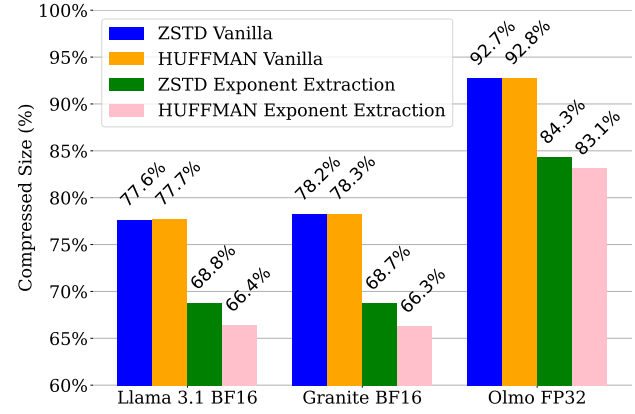


Figure 4. Breakdown of the contributions of Exponent Extraction and Huffman only encoding to compression ratio.

When compressing regular models we found that the exponent compresses by approximately a 3X factor (namely compressed size of 33%) whereas the fraction and sign bits hardly compress at all. The overall savings is thus dictated by the weight of the exponent in the parameter. That is, for BF16 the compressed size is $\frac{1}{2} \cdot 33.3 + \frac{1}{2} \cdot 100 \approx 66.6$, whereas for FP32 it is $\frac{1}{4} \cdot 33.3 + \frac{3}{4} \cdot 100 \approx 83.3$. As a result, the main benefit of compressing regular models lies in BF16 models (which fortunately are most of the new models used in practice). We show the effect on performance of the exponent extraction and Huffman only encoding in Section 5.2

3.2 Compressing Clean Models

As mentioned earlier, most models only show compressibility in the exponent. However, we also see some models that are surprisingly more compressible, and show compressibility also in the fraction part of the parameters. We call these clean models, since after further fine tuning they typically lose their extra compressibility. That being said, these include some very popular models, such as Bge, RoBERTa, Xlm-RoBERTa, Whisper, and Clip.

Clean models pose some additional challenges in devising the best possible compression method for models. While for regular models one can assume the fraction is incompressible and not compress it, for general models we need to identify that the fraction is indeed compressible and furthermore, choose the correct compression method for the fraction part. We first describe our observations regarding how to best compress clean models.

Byte Grouping. When dealing with FP32 models, the first observation regarding fraction compression is that also within the fraction different bytes have different compressibility. For example, if rounding is used, then the least bits of the fraction will be zeros while the most bits will remain more or less random. This suggests that the different bytes of the fraction should also be separated into different compression streams. We call this technique *byte grouping* and it is depicted in Figure 5.

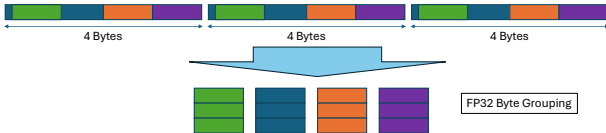


Figure 5. An example of Byte Grouping for FP32. The first group consists of the exponents. The rest of the data is split into 3 groups, one per each byte in the parameter.

Like the exponent, Huffman only decoding wins out for the byte groups that are compressible except for all zero streams that can simply be truncated and replaced by a header (the Huffman implementation that we use does this automatically). Figure 6 shows an example of the effect of compressing a clean model (xlm-RoBERTa), with and without byte grouping. When the fraction is broken down into bytes we see different behavior for the different byte groups. Byte 1 is barely compressible, while byte 3, being all zeros, is highly compressed. Byte 2 is quite compressible and compresses a little better with Huffman only.

Identifying compressibility. Identifying incompressible data in advance has the benefit of speeding up compression

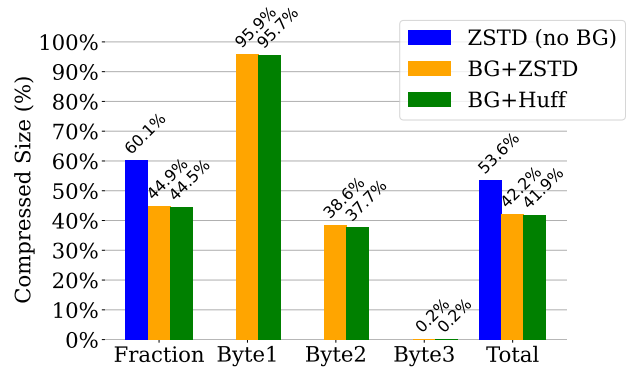


Figure 6. Compression ratios for the clean model xlm-RoBERTa (FP32) with and without byte grouping (BG), including a breakdown of compressibility of the 3 fraction bytes. Total includes the fraction and exponent parts.

time. Various methods have been discussed in prior work to achieve this, e.g. (Harnik et al., 2013). We propose a simple method that builds on the fact that within each byte group compressibility seems to be consistent. We compress a chunk, and if it is not compressible we skip the compressibility of the following few chunks before trying to compress again (the specific number varies with the actual implementation). The rationale in retrying to compress is to identify a possible change in behavior between different layers or parts of the model.

3.3 Compressibility summary

Table 2 presents the compressibility of various models using ZipNN with a breakdown of compressibility of the various byte groups. The first byte group consists of the exponent. We see all BF16 models achieve a space saving of about $\frac{1}{3}$ of the model size. Regular models with parameter types FP32 or FP16 show less impressive space savings whereas clean models of these type show much better space savings. In clean FP32 models byte grouping plays a key role as seen in the breakdown. We also see clean models in the FP16 family that are likely the result of transformation from BF16 models (which has a shorter fraction part than FP16).

4 BEYOND MODEL COMPRESSION

So far we focused only on compression of full models in standalone form. In this section, we discuss how our methods fare when compressing artifacts of the training process, including Optimizer, Gradient and checkpointing data.

MODEL NAME	PARAM TYPE	MODEL SIZE	COMPRESSED SIZE	BREAKDOWN TO BYTE GROUP
FALCON-7B	BF16	14.4 GB	66.4%	(32.8%, 100%)
BLOOM	BF16	328.2 GB	67.4%	(34.8%, 100%)
OPENLLAMA-3B	BF16	6.9 GB	66.4%	(32.7%, 100%)
MISTRAL	BF16	14.5 GB	66.3%	(32.5%, 100%)
LLAMA-3.1	BF16	16 GB	66.4%	(32.8%, 99.9%)
WAV2VEC	FP32	1.2 GB	83.3%	(33.0%, 100%, 100%, 100%)
BERT	FP32	0.4 GB	83.0%	(32.6%, 99.5%, 100%, 100%)
OLMO	FP32	5.1 GB	83.1%	(32.5%, 100%, 100%, 100%)
STABLE-VIDEO-DIFFUSION	FP16	4.27 GB	84.8%	(69.6%, 100%)
CAPYBARAHERMES-MISTRAL	FP16	14.5 GB	84.4%	(68.8%, 100%)
XLM-ROBERTA	FP32	1.1 GB	41.8%	(33.9%, 95.6%, 37.5%, 0.0%)
CLIP	FP32	1.7 GB	48.1%	(33.1%, 100%, 45.9%, 13.4%)
T5 BASE	FP32	0.8 GB	33.7%	(34.6%, 100%, 0.0%, 0.0%)
LLAMA2-13B	FP16	26 GB	66.6%	(64.2%, 69.0%)
TULU-7B	FP16	13.5 GB	66.6%	(64.2%, 68.9%)

Table 2. Compressed size for various Models with ZipNN method with Byte Grouping. Based on compressing 1GB from the middle of a model (for large models), and the entire model, excluding the first 10MB (headers etc...) for smaller models.

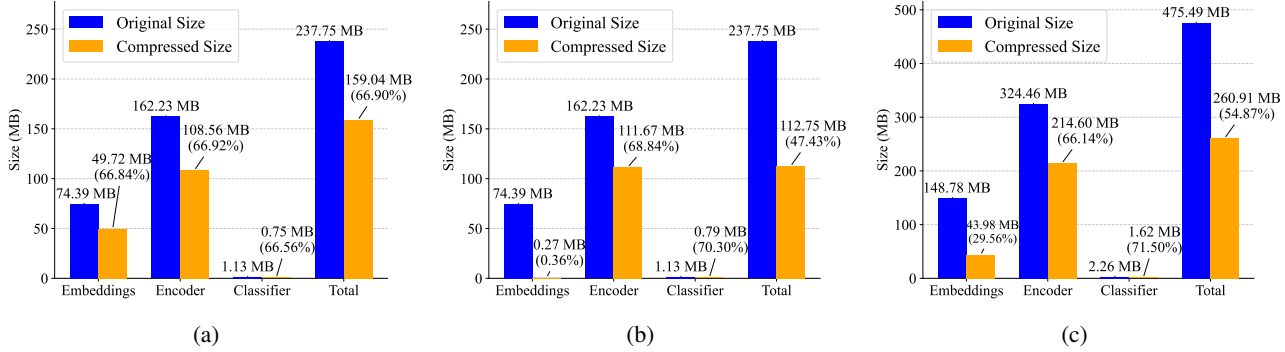


Figure 7. Compressibility of the various layers in the Roberta Model (a), Gradients (b) and Optimizer (c) during training. Compression for all layers uses exponent extraction. The embedding layer in the gradients and optimizers is then compressed using Zstd while all other layers use Huffman.

4.1 Gradients and Optimizers

Gradients and Optimizers are derivatives of the training process. These artifacts are required in order to continue the training process and as such take up substantial network bandwidth (in the case of distributed training) or storage space (in the case of checkpoints). Gradients and Optimizers are often of equal in size to the models (Anil et al., 2020) and therefore can also benefit from compression.

We investigate a BF16 version of RoBERTa under finetuning and generate intermediate gradients and optimizers, as well as the model itself. Interestingly, we found that gradients and optimizers compress better than the actual model. While the model compressed size is, as expected, around 66%, the optimizer is at 54% and gradient at 47%. The source of the extra compressibility is found in the different

layers of the model. Figure 7 shows a breakdown of the compressibility in the various model layers. Interestingly, the token embeddings layer is extremely compressible in the gradients and optimizers, whereas in the model itself, this layer is not different than other layers. The general layers in optimizers and gradient compress to around 66%, slightly better than these layers in the model itself. In addition, we find that both in gradients and optimizers, the embedding layer is compressed significantly better with Zstd (unlike the model itself).

4.2 Checkpoints and Delta Compression

When models have high similarity, one strategy to optimize storage and network transfer is to save a base model and for the rest of the models only store the differences from this

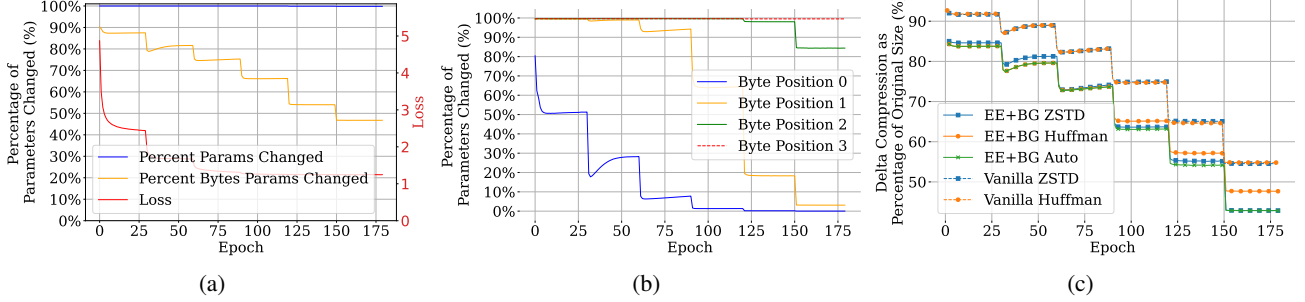


Figure 8. Resnet 18 finetuning test with checkpoints taken every epoch. (a) shows the amount of change in parameters and bytes as a function of epoch; (b) breaks down this change according to byte groups; (c) shows the delta compression effectiveness with various techniques. The steps seen in the graphs coincide with the steps of the learning rate scheduler.

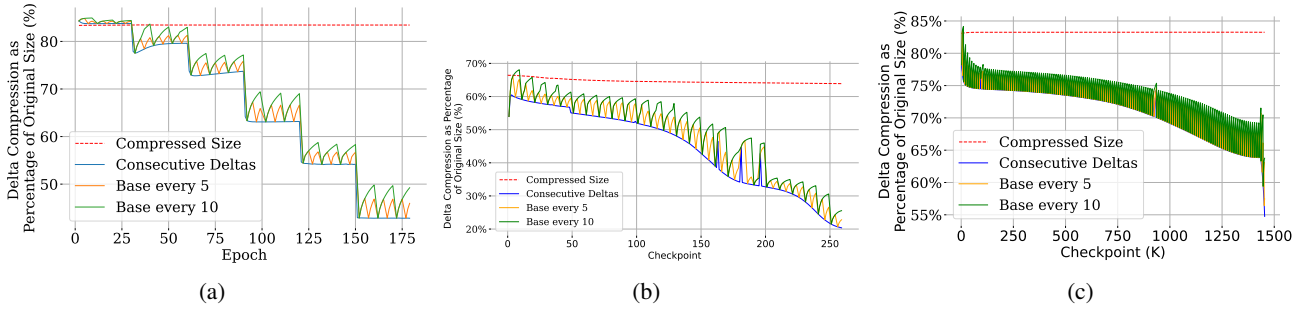


Figure 9. Compression of checkpoints with periodic bases for (a) ResNet (FP32); (b) Amber (BF16); and (c) Olmo (FP32). In the graphs, we ignore the space of the periodic full bases.

base model (Kandpal et al., 2023). We refer to compressing those differences as *delta compression*. To reconstruct a model, one only needs to apply the delta to the base model. A straightforward approach to delta compression is to compute the difference between the two models (e.g. using XOR or subtraction) and compress this delta using a lossless compressor. In our work, we used XOR for the delta as it is easily reversible and does not require any extra bits. A natural use case in which delta compression proves very useful is checkpointing. In checkpointing, we repeatedly store models that have limited change between them. Fine tuning often changes models in small quantities. Hence the delta between the results of consecutive training epochs has the potential to be more compressible than stand-alone models. We studied this while finetuning a Resnet 18 model (FP32). Figure 8(a) shows the amount of change between consecutive checkpoints as the process progresses and the loss function drops. We see that while all parameters in the model change in each epoch, when broken down to bytes, more and more bytes remain unchanged as the training converges. Figure 8(b) breaks this down according to byte groups. Here we see that the exponent byte has the least changes, whereas the least bits in the fraction have the

most change. All byte groups show a growing number of steady bytes as the training converges. This suggests that byte grouping is helpful for delta compression as well, as our tests in Figure 8(c) corroborate.

Auto Detection of Compression method. While investigating compressibility of deltas, we realized that at some point it is worthwhile to compress the delta using Zstd over Huffman. This is mostly a function of the number of zeros in the delta (unchanged bytes). For this purpose we devised an auto-selection mechanism that decides between Huffman and Zstd based on two criteria. For each chunk, ZipNN counts the number of zeros in the chunk, as well as the length of the longest zero sequence. By running a simulation we found that Zstd compresses better than Huffman if the number of zeros exceeds 90%. It also outperforms Huffman if there is any long sequence of zeros (which may happen if certain layers are ruled as non-modifiable by the training mechanism) and we set the detection level at 3% of the chunk size. Figure 8(c) also compares running with Huffman, vs. Zstd vs. the Auto detection method. We see that Huffman outperforms Zstd in the first two steps of the learning rate scheduler, and this flips after the 3rd step. Auto

manages to pick correctly and is always at least as good as the better method.

Periodic Base. A major drawback of delta compression is that in order to recover a checkpoint one must obtain both the base and the delta. But if the checkpoints are all stored using delta compression, this would result in long chains of deltas, making the recovery process prohibitively expensive. Instead, it is customary to periodically store a full checkpoint (compressed standalone), serving as a base for the next k checkpoints. Suppose that we store a base every 10 checkpoints, then the longest chain of deltas would be of length 9. Another approach is to store a periodical base and always do the delta with respect to the last full base. This means that there are never delta chains, but rather only pairs of base and delta. On the other hand, if the period is for example 10, we may be doing a delta against a base that is 9 epochs ago, and may achieve worst delta compression. In Figure 9 we study what the compression would be if we use a periodic base for a period of 5 and 10. We use the self trained ResNet18 as well as two models for which training checkpoints have been made public (Amber and Olmo). Depending on the model and the epoch we see that using a base at distance 5 or even 10, while not as optimal as consecutive deltas, is still far better than standalone compression.

Another use-case is when a hub or user stores multiple models with high similarity (regardless of checkpointing). One source for such occurrence is when multiple models are trained or fine tuned from the same base model. For example, we found in Hugging Face 3 variations of RoBERTa trained on tweets which are tuned for different purposes - detecting irony, detecting offensive language, and detecting abuse. As standalone models, their compressed size is 83.7% on average. However, compressing the delta of each of the pairs achieves a compressed size of 56% on average.

5 IMPLEMENTATION AND EVALUATION

5.1 Implementation

We implemented our method and it is now an open source project ([ZipNN](#)). Its core is written in C (2000 lines of code) and the wrappers, scripts and tests are all written in Python (4000 lines of code). We use the Zstd v1.5.6 library as well as Zstd's underlying Huffman implementation as the underlying compressors. For our tests in Python, we use zstandard 0.23.0, torch 2.4.0, and numpy 2.1.0.

Chunking. When designing our method, we aimed to create an implementation that could process small chunks independently, allowing each chunk to be handled in parallel. This architecture is ideal for GPUs, which contain many cores that, while less powerful than CPU cores, excel in concurrent tasks. Our implementation includes two levels

of granularity: **chunk level** and **byte-group level** within each chunk. By default, each chunk is of size 256KB. In the BF16 format byte-groups are sized at 128KB whereas in FP32 byte-groups are of size 64KB. Parallelism can be conducted at the chunk level, and we also parallelize the byte-group compression/decompression processes. Auto decisions on compression method can be done at a byte-group granularity.

Metadata and parallelism. During compression, due to the fixed-sized compression chunks, one can easily parallelize the compression process to multiple workers. However, during decompression, the chunks are of variable size. To enable parallel processing, we add a map for the whole model containing metadata for each byte-group and each chunk.

Hugging Face Integration. For smooth integration with Hugging Face's Transformers library ([Wolf et al., 2020](#)), we implemented a mechanism that automatically decompresses downloaded models, reorders symbolic links in the local cache, updates metadata, and removes the compressed files. We also included an option for manual compression or decompression of models in the local cache.

5.2 Compression and Decompression speed

We ran our tests on an Apple M1 Max machine with 10 cores and 64GB of RAM running macOS Sonoma 14.3. The tests run in a single process and on a single core. Table 3 shows the speed benefits of our method vs. vanilla compressors on 3 representative models. Two regular models (BF16 and FP32) and one clean model (FP32). The exponent-extraction and byte grouping carry a performance penalty, that is amplified by the fact that the compressor works harder if it actually manages to find some repetitions, yet the use of Huffman only encoding makes up for this and we manage to improve both on speed and on compression ratio simultaneously.

The variation in speeds between the various models is also explained by their compressibility. While in the regular FP32 model $\frac{3}{4}$ of the model is non compressible and mostly skipped, in the BF16 this is only $\frac{1}{2}$ and in the clean model even less than that. Note that we tested LZ4 and Snappy on these models and while they are faster than all methods, they gain zero compression savings.

5.3 End-2-End Evaluation

In this section, we focus on time aspects and end-2-end timing of our first use-case - that of model hubs. We measured the time it takes to upload and download from Hugging Face to a virtual machine that runs on one of the cloud providers and is located in the Milan region. We also measured upload and download performance on a home laptop with a

Model name	Comp. method	Comp. size (%)	Comp. speed (GB/Sec)	Decomp. speed (GB/Sec)
Llama-3.1	Zstd	77.7	0.71	1.02
	EE+Zstd	68.8	0.51	1.21
	ZipNN	66.4	1.15	1.65
Olmo-1b	Zstd	92.3	0.97	1.02
	FP32	84.4	0.82	1.97
	ZipNN	83.2	1.64	2.48
xlm-RoBERTa	Zstd	57.4	0.18	0.77
	EE+Zstd	46.7	0.42	0.89
	FP32	42.9	0.83	1.41

Table 3. Comparing speeds of compression methods on two regular models. Zstd was used with default configuration. Our method, ZipNN, consists of Exponent-Extraction and Huffman only compression. EE-Zstd denotes Exponent-Extraction with Zstd compression on the exponent. Based on 10 runs on 1GB from the middle of the model. The maximum standard deviation was 2%.

500Mbps network.

Unlike storage benefits, communication speeds depend heavily on the medium. We first characterized the general behavior of the communication with the Hugging Face hub. The upload bandwidth observed in the cloud remained mostly constant (at around 20 MBps). For downloads, we observed 2 types of data transfer speeds.

First Download - The speed in the first download showed large variance. On the cloud VM we measured 20-40 MBps. The home machine achieved approximately 10MBps.

Cached Download - The second read on the data is likely downloaded from a cloud cache and exhibits speed of 120-130 MBps on the cloud VM and approximately 40MBps at the home location.

The end-2-end timing behavior is dictated by the time to compress/decompress the model and the time to upload/download it respectively. We measured timing with lossless compression on the 3 representative models tested in the previous section. Figure 10 shows the timing of upload and download speeds of the three models. Each test was run 10 times for the cached reads and 5 times for the 1st timers. The variance was almost entirely due to the network time and this standard deviation is depicted in the graph. The actual compression and decompression time had very little variance. For example, for the xlm-RoBERTa model the average time for the decompression was 3.92 seconds with a standard deviation of 0.017.

As expected, highly compressible models show significant time improvements whereas the less compressible models show more modest time savings. Naturally, the time saving

is more significant when the network is slower. The upload time improves greatly since the bandwidth for uploads is low. On the other hand, the upload savings are lower than download with similar bandwidth reflecting the fact that compression is slower than decompression.

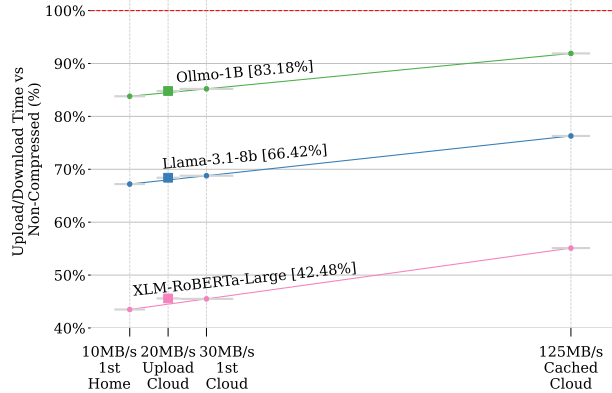


Figure 10. Download and upload times of 3 models using our compression vs. the non-compressed version.

6 RELATED WORK

6.1 Model Compression

In the literature, "model-compression" is a field of its own, aimed at creating smaller models that mimic the original model. Model-compression is hence the name for a set of tools that aim to *accelerate* models, usually at inference, by reducing their size (Choudhary et al., 2020). Under such conditions, a method is allowed to reduce the accuracy, and is judged on its tradeoff between size and performance. This differs from lossless compression which is supposed to return the model to its original state after decompression.

There are four main methods to reduce model size in that manner (Choudhary et al., 2020). Pruning (LeCun et al., 1989; Hanson & Pratt, 1988; Zhu & Gupta, 2017) (sometimes referred to as sparsification; (Ma et al., 2021)) where parts of the model are removed, dedicated training or network architecture (Oktay et al., 2019), distillation (Gou et al., 2021) or otherwise training a smaller model from a better model (Haroush et al., 2019), and quantization (Gholami et al., 2021). There are also methods that combine several of those (Polino et al., 2018), including the only work we have found to propose compression, which it applies after two other model-compression steps (Han et al., 2015).

Out of the model-compression techniques, quantization (Gray, 1984) is perhaps the most popular. Quantization is a method that bins weight values to a more coarse granularity. By design it trades-off accuracy for space and speed and is hence a lossy compression technique. Quantization is bound to increase the amount of entropy per byte in a model but is not trying to push it to the limit. As such, quan-

itized models can potentially be further compressed using lossless compression. We see mixed results: with some off-the-shelf quantized models that have been quantized with GTPQ (Frantar et al., 2022) and AWQ (Lin et al., 2023) we find that they are still compressible, with a compressed size between 85-91%. On the other hand, we found that other quantized models using GGUF do not compress at all.

6.2 Other Related Work

Similar to delta compression some works analyze dimensionality (Aghajanyan et al., 2021; Gueta et al., 2023) or save the deltas for actions such as compositionally (Ilharco et al., 2022) and merging multiple deltas (Choshen et al., 2022; Wortsman et al., 2022; Matena & Raffel, 2021). Few works also apply on such deltas methods like pruning (Yadav et al., 2023), trained sparsity (Zhang et al., 2023) or quantization (Dettmers et al., 2023) or discuss deltas.

Another line of work worth mentioning is computation graph optimization (Sabne, 2020; Wu, 2023). Such works reduce the computation graph and perform optimization there. It is noteworthy to contrast it to our work. such work compresses the size of the computation graph, which speeds computation, but does not change the model weights, and it is hence orthogonal to our work. To validate that, we compressed pyTorch (Wu, 2023) models before and after compilation, finding compression works similarly well.

Last, related to the optimization process (see §4.1), a few recent works offer to reduce the information passed in gradient updates hence making them faster, further overcoming the decrease in information per example by seeing more examples per second (Tyagi & Swany, 2023; Zhao et al., 2024).

7 CONCLUSION

We are in an era where models and system requirements grow larger – overparametrization seems to be beneficial for better learning. As our compression findings hint, this overparametrization is not fully used for inference or for the weights themselves and there is redundancy. Hence the wide attention and progress made to reducing model sizes is not without merit. That being said, the reality is that commonly used models are not kept or run in reduced form and there is great inefficiency in the way models are stored and communicated today. Some of this inefficiency can be mitigated using the compression techniques outlined in this paper. Even more so, by tailoring our compression to models, one can achieve significantly better compression with significantly smaller overhead.

Given the reduction in network bandwidth, storage, and time, we think that lossless compression should be the default in communication with model hubs such as Hug-

ging Face. Moreover, we believe that communication compression has multiple other use-cases in the realm of training, versioning, and serving models.

REFERENCES

Adler, M. and Gailly, J.-L. Zlib, 2024. URL <https://www.zlib.net/>.

Aghajanyan, A., Gupta, S., and Zettlemoyer, L. Intrinsic dimensionality explains the effectiveness of language model fine-tuning. In Zong, C., Xia, F., Li, W., and Navigli, R. (eds.), *Proceedings of the 59th Annual Meeting of the Association for Computational Linguistics and the 11th International Joint Conference on Natural Language Processing (Volume 1: Long Papers)*, pp. 7319–7328, Online, August 2021. Association for Computational Linguistics. doi: 10.18653/v1/2021.acl-long.568. URL <https://aclanthology.org/2021.acl-long.568>.

Almazrouei, E., Alobeidli, H., Alshamsi, A., Cappelli, A., Cojocaru, R., Debbah, M., Goffinet, E., Heslow, D., Lainay, J., Malartic, Q., Noune, B., Pannier, B., and Penedo, G. Falcon-40B: an open large language model with state-of-the-art performance. 2023.

Anil, R., Gupta, V., Koren, T., Regan, K., and Singer, Y. Scalable second order optimization for deep learning. *arXiv preprint arXiv:2002.09018*, 2020.

Baevski, A., Zhou, H., Mohamed, A., and Auli, M. wav2vec 2.0: A framework for self-supervised learning of speech representations, 2020.

Biderman, S., Schoelkopf, H., Anthony, Q. G., Bradley, H., O’Brien, K., Hallahan, E., Khan, M. A., Purohit, S., Prashanth, U. S., Raff, E., Skowron, A., Sutawika, L., and van der Wal, O. Pythia: A suite for analyzing large language models across training and scaling. *ArXiv*, abs/2304.01373, 2023. URL <https://api.semanticscholar.org/CorpusID:257921893>.

Blattmann, A., Dockhorn, T., Kulal, S., Mendelevitch, D., Kilian, M., Lorenz, D., Levi, Y., English, Z., Voleti, V., Letts, A., et al. Stable video diffusion: Scaling latent video diffusion models to large datasets. *arXiv preprint arXiv:2311.15127*, 2023.

Choshen, L., Venezian, E., Slonim, N., and Katz, Y. Fusing finetuned models for better pretraining. *ArXiv*, abs/2204.03044, 2022.

Choudhary, T., Mishra, V., Goswami, A., and Sarangapani, J. A comprehensive survey on model compression and acceleration. *Artificial Intelligence Review*, 53:5113–5155, 2020.

Collet, Y. Lz4 - extremely fast compression, 2024a. URL <https://github.com/lz4/lz4>.

Collet, Y. Zstandard, 2024b. URL <https://github.com/facebook/zstd>.

Collet, Y. and Kucherawy, M. Zstandard compression and the application/zstd media type. Technical report, 2018.

Conneau, A., Khandelwal, K., Goyal, N., Chaudhary, V., Wenzek, G., Guzmán, F., Grave, E., Ott, M., Zettlemoyer, L., and Stoyanov, V. Unsupervised cross-lingual representation learning at scale. *CoRR*, abs/1911.02116, 2019. URL <http://arxiv.org/abs/1911.02116>.

Dean, J., Ghemawat, S., and Gunderson, S. H. Snappy, a fast compressor/decompressor., 2024. URL <https://github.com/google/snappy>.

Dettmers, T., Pagnoni, A., Holtzman, A., and Zettlemoyer, L. Qlora: Efficient finetuning of quantized llms. *arXiv preprint arXiv:2305.14314*, 2023.

Deutsch, P. and Gailly, J.-L. Zlib compressed data format specification version 3.3. Technical report, 1996.

Devlin, J., Chang, M.-W., Lee, K., and Toutanova, K. Bert: Pre-training of deep bidirectional transformers for language understanding. In *North American Chapter of the Association for Computational Linguistics*, 2019. URL <https://api.semanticscholar.org/CorpusID:52967399>.

Diskin, M., Bukhriyarov, A., Ryabinin, M., Saulnier, L., lhoest, q., Sinitin, A., Popov, D., Pyrkin, D. V., Kashirin, M., Borzunov, A., Villanova del Moral, A., Mazur, D., Kobelev, I., Jernite, Y., Wolf, T., and Pekhimenko, G. Distributed deep learning in open collaborations. In Ranzato, M., Beygelzimer, A., Dauphin, Y., Liang, P., and Vaughan, J. W. (eds.), *Advances in Neural Information Processing Systems*, volume 34, pp. 7879–7897. Curran Associates, Inc., 2021. URL https://proceedings.neurips.cc/paper_files/paper/2021/file/41a60377ba920919939d83326ebbe5a1-Paper.pdf.

Dodge, J., Ilharco, G., Schwartz, R., Farhadi, A., Hajishirzi, H., and Smith, N. A. Fine-tuning pre-trained language models: Weight initializations, data orders, and early stopping. *ArXiv*, abs/2002.06305, 2020. URL <https://api.semanticscholar.org/CorpusID:211132951>.

Don-Yehiya, S., Venezian, E., Raffel, C., Slonim, N., and Choshen, L. ColD fusion: Collaborative descent for distributed multitask finetuning. In Rogers, A., Boyd-Graber, J., and Okazaki, N. (eds.), *Proceedings of the 61st Annual Meeting of the Association for Computational Linguistics (Volume 1: Long Papers)*, pp. 788–806, Toronto, Canada, July 2023. Association for Computational Linguistics. doi: 10.18653/v1/2023.acl-long.46. URL <https://aclanthology.org/2023.acl-long.46>.

Dubey, A., Jauhri, A., Pandey, A., Kadian, A., Al-Dahle, A., Letman, A., Mathur, A., Schelten, A., Yang, A., Fan, A., et al. The llama 3 herd of models. *arXiv preprint arXiv:2407.21783*, 2024.

Fedus, W., Zoph, B., and Shazeer, N. M. Switch transformers: Scaling to trillion parameter models with simple and efficient sparsity. *J. Mach. Learn. Res.*, 23:120:1–120:39, 2021. URL <https://api.semanticscholar.org/CorpusID:231573431>.

Frantar, E., Ashkboos, S., Hoefer, T., and Alistarh, D. Gptq: Accurate post-training quantization for generative pre-trained transformers. *arXiv preprint arXiv:2210.17323*, 2022.

Geng, X. and Liu, H. Openllama: An open reproduction of llama, May 2023. URL https://github.com/openlm-research/open_llama.

Gholami, A., Kim, S., Dong, Z., Yao, Z., Mahoney, M. W., and Keutzer, K. A survey of quantization methods for efficient neural network inference, 2021.

Google. Tensorflow hub, 2018. URL <https://www.tensorflow.org/hub>.

Gou, J., Yu, B., Maybank, S. J., and Tao, D. Knowledge distillation: A survey. *International Journal of Computer Vision*, 129:1789–1819, 2021.

Granite Team, I. Granite 3.0 language models, 2024.

Gray, R. Vector quantization. *IEEE Assp Magazine*, 1(2): 4–29, 1984.

Groeneveld, D., Beltagy, I., Walsh, P., Bhagia, A., Kinney, R., Tafjord, O., Jha, A. H., Ivison, H., Magnusson, I., Wang, Y., Arora, S., Atkinson, D., Author, R., Chandu, K., Cohan, A., Dumas, J., Elazar, Y., Gu, Y., Hessel, J., Khot, T., Merrill, W., Morrison, J., Muennighoff, N., Naik, A., Nam, C., Peters, M. E., Pyatkin, V., Ravichander, A., Schwenk, D., Shah, S., Smith, W., Subramani, N., Wortsman, M., Dasigi, P., Lambert, N., Richardson, K., Dodge, J., Lo, K., Soldaini, L., Smith, N. A., and Hajishirzi, H. Olmo: Accelerating the science of language models. *Preprint*, 2024.

Gueta, A., Venezian, E., Raffel, C., Slonim, N., Katz, Y., and Choshen, L. Knowledge is a region in weight space for fine-tuned language models. In Bouamor,

H., Pino, J., and Bali, K. (eds.), *Findings of the Association for Computational Linguistics: EMNLP 2023*, pp. 1350–1370, Singapore, December 2023. Association for Computational Linguistics. doi: 10.18653/v1/2023. findings-emnlp.95. URL <https://aclanthology.org/2023.findings-emnlp.95>.

Han, S., Mao, H., and Dally, W. J. Deep compression: Compressing deep neural network with pruning, trained quantization and huffman coding. *arXiv: Computer Vision and Pattern Recognition*, 2015. URL <https://api.semanticscholar.org/CorpusID:2134321>.

Hanson, S. J. and Pratt, L. Y. Comparing biases for minimal network construction with back-propagation. In *Neural Information Processing Systems*, 1988. URL <https://api.semanticscholar.org/CorpusID:9344018>.

Harnik, D., Kat, R., Sotnikov, D., Traeger, A., and Margalit, O. To zip or not to zip: Effective resource usage for Real-Time compression. In *11th USENIX Conference on File and Storage Technologies (FAST 13)*, pp. 229–241, San Jose, CA, February 2013. USENIX Association. ISBN 978-1-931971-99-7. URL <https://www.usenix.org/conference/fast13/technical-sessions/presentation/harnik>.

Haroush, M., Hubara, I., Hoffer, E., and Soudry, D. The knowledge within: Methods for data-free model compression. *2020 IEEE/CVF Conference on Computer Vision and Pattern Recognition (CVPR)*, pp. 8491–8499, 2019. URL <https://api.semanticscholar.org/CorpusID:208548669>.

He, K., Zhang, X., Ren, S., and Sun, J. Deep residual learning for image recognition. In *Proceedings of the IEEE conference on computer vision and pattern recognition*, pp. 770–778, 2016.

Huffman, D. A. A method for the construction of minimum-redundancy codes. *Proceedings of the IRE*, 40(9):1098–1101, 1952. doi: 10.1109/JRPROC.1952.273898.

Ilharco, G., Ribeiro, M. T., Wortsman, M., Gururangan, S., Schmidt, L., Hajishirzi, H., and Farhadi, A. Editing models with task arithmetic. *arXiv preprint arXiv:2212.04089*, 2022.

Ivison, H., Wang, Y., Pyatkin, V., Lambert, N., Peters, M., Dasigi, P., Jang, J., Wadden, D., Smith, N. A., Beltagy, I., and Hajishirzi, H. Camels in a changing climate: Enhancing lm adaptation with tulu 2, 2023.

Jiang, A. Q., Sablayrolles, A., Mensch, A., Bamford, C., Chaplot, D. S., Casas, D. d. l., Bressand, F., Lengyel, G., Lample, G., Saulnier, L., et al. Mistral 7b. *arXiv preprint arXiv:2310.06825*, 2023.

Junczys-Dowmunt, M., Grundkiewicz, R., Dwojak, T., Hoang, H. T., Heafield, K., Neckermann, T., Seide, F., Germann, U., Aji, A. F., Bogoychev, N., Martins, A. F. T., and Birch, A. Marian: Fast neural machine translation in c++. In *Annual Meeting of the Association for Computational Linguistics*, 2018. URL <https://api.semanticscholar.org/CorpusID:4623739>.

Kandpal, N., Lester, B., Muqeeth, M., Mascarenhas, A., Evans, M., Baskaran, V., Huang, T., Liu, H., and Raffel, C. Git-theta: A git extension for collaborative development of machine learning models. *arXiv preprint arXiv:2306.04529*, 2023.

LeCun, Y., Denker, J. S., and Solla, S. A. Optimal brain damage. In *Neural Information Processing Systems*, 1989. URL <https://api.semanticscholar.org/CorpusID:7785881>.

Li, M., Gururangan, S., Dettmers, T., Lewis, M., Althoff, T., Smith, N. A., and Zettlemoyer, L. Branch-train-merge: Embarrassingly parallel training of expert language models. *arXiv preprint arXiv:2208.03306*, 2022.

Lialin, V., Muckatira, S., Shivagunde, N., and Rumshisky, A. Relora: High-rank training through low-rank updates. In *Workshop on Advancing Neural Network Training: Computational Efficiency, Scalability, and Resource Optimization (WANT@ NeurIPS 2023)*, 2023.

Lin, J., Tang, J., Tang, H., Yang, S., Dang, X., and Han, S. Awq: Activation-aware weight quantization for llm compression and acceleration. *arXiv preprint arXiv:2306.00978*, 2023.

Liu, Y., Ott, M., Goyal, N., Du, J., Joshi, M., Chen, D., Levy, O., Lewis, M., Zettlemoyer, L., and Stoyanov, V. Roberta: A robustly optimized BERT pretraining approach. *CoRR*, abs/1907.11692, 2019a. URL <http://arxiv.org/abs/1907.11692>.

Liu, Y., Ott, M., Goyal, N., Du, J., Joshi, M., Chen, D., Levy, O., Lewis, M., Zettlemoyer, L., and Stoyanov, V. Roberta: A robustly optimized bert pretraining approach. *arXiv preprint arXiv:1907.11692*, 2019b.

Liu, Z., Qiao, A., Neiswanger, W., Wang, H., Tan, B., Tao, T., Li, J., Wang, Y., Sun, S., Pangarkar, O., Fan, R., Gu, Y., Miller, V., Zhuang, Y., He, G., Li, H., Koto, F., Tang, L., Ranjan, N., Shen, Z., Ren, X., Iriondo, R., Mu, C., Hu, Z., Schulze, M., Nakov, P., Baldwin, T., and Xing, E. P. Llm360: Towards fully transparent open-source llms. *arXiv*, 2023.

Ma, X., Qin, M., Sun, F., Hou, Z., Yuan, K., Xu, Y., Wang, Y., Chen, Y.-K., Jin, R., and Xie, Y. Effective model sparsification by scheduled grow-and-prune methods. *arXiv preprint arXiv:2106.09857*, 2021.

Matena, M. and Raffel, C. Merging models with fisher-weighted averaging. *arXiv preprint arXiv:2111.09832*, 2021.

Oktay, D., Ballé, J., Singh, S., and Shrivastava, A. Scalable model compression by entropy penalized reparameterization. *arXiv preprint arXiv:1906.06624*, 2019.

Pfeiffer, J., Rücklé, A., Poth, C., Kamath, A., Vulić, I., Ruder, S., Cho, K., and Gurevych, I. AdapterHub: A framework for adapting transformers. In Liu, Q. and Schlangen, D. (eds.), *Proceedings of the 2020 Conference on Empirical Methods in Natural Language Processing: System Demonstrations*, pp. 46–54, Online, October 2020. Association for Computational Linguistics. doi: 10.18653/v1/2020.emnlp-demos.7. URL <https://aclanthology.org/2020.emnlp-demos.7>.

Polino, A., Pascanu, R., and Alistarh, D. Model compression via distillation and quantization. *arXiv preprint arXiv:1802.05668*, 2018.

Pytorch. Pytorch hub, 2019. URL <https://pytorch.org/hub/>.

Qualcomm AI Hub. Qualcomm® ai hub. <https://aihub.qualcomm.com/>.

Radford, A., Kim, J. W., Hallacy, C., Ramesh, A., Goh, G., Agarwal, S., Sastry, G., Askell, A., Mishkin, P., Clark, J., Krueger, G., and Sutskever, I. Learning transferable visual models from natural language supervision, 2021. URL <https://arxiv.org/abs/2103.00020>.

Radford, A., Kim, J. W., Xu, T., Brockman, G., McLeavey, C., and Sutskever, I. Robust speech recognition via large-scale weak supervision, 2022. URL <https://arxiv.org/abs/2212.04356>.

Raffel, C., Shazeer, N., Roberts, A., Lee, K., Narang, S., Matena, M., Zhou, Y., Li, W., and Liu, P. J. Exploring the limits of transfer learning with a unified text-to-text transformer. *The Journal of Machine Learning Research*, 21(1):5485–5551, 2020.

Rissanen, J. J. Generalized kraft inequality and arithmetic coding. *IBM Journal of Research and Development*, 20 (3):198–203, 1976. doi: 10.1147/rd.203.0198.

Sabne, A. Xla: Compiling machine learning for peak performance. 2020.

Sandler, M., Zhmoginov, A., Vladymyrov, M., and Miller, N. Training trajectories, mini-batch losses and the curious role of the learning rate. *ArXiv*, abs/2301.02312, 2023. URL <https://api.semanticscholar.org/CorpusID:255522706>.

Shoeybi, M., Patwary, M., Puri, R., LeGresley, P., Casper, J., and Catanzaro, B. Megatron-lm: Training multi-billion parameter language models using model parallelism. *arXiv preprint arXiv:1909.08053*, 2019.

Song, K., Tan, X., Qin, T., Lu, J., and Liu, T. Mpnet: Masked and permuted pre-training for language understanding. *CoRR*, abs/2004.09297, 2020. URL <https://arxiv.org/abs/2004.09297>.

Squash. Squash compression benchmark, 2016. URL <http://quixdb.github.io/squash-benchmark/>.

Team, Q. Qwen2.5: A party of foundation models, September 2024. URL <https://qwenlm.github.io/blog/qwen2.5/>.

Touvron, H., Martin, L., Stone, K., Albert, P., Almahairi, A., Babaei, Y., Bashlykov, N., Batra, S., Bhargava, P., Bhosale, S., et al. Llama 2: Open foundation and fine-tuned chat models. *arXiv preprint arXiv:2307.09288*, 2023.

Turner, R., Eriksson, D., McCourt, M. J., Kiili, J., Laaksonen, E., Xu, Z., and Guyon, I. M. Bayesian optimization is superior to random search for machine learning hyperparameter tuning: Analysis of the black-box optimization challenge 2020. In *Neural Information Processing Systems*, 2021. URL <https://api.semanticscholar.org/CorpusID:233324399>.

Tyagi, S. and Swany, M. Gravac: Adaptive compression for communication-efficient distributed dl training. In *2023 IEEE 16th International Conference on Cloud Computing (CLOUD)*, pp. 319–329. IEEE, 2023.

Wang, P., Bai, S., Tan, S., Wang, S., Fan, Z., Bai, J., Chen, K., Liu, X., Wang, J., Ge, W., Fan, Y., Dang, K., Du, M., Ren, X., Men, R., Liu, D., Zhou, C., Zhou, J., and Lin, J. Qwen2-vl: Enhancing vision-language model’s perception of the world at any resolution. *arXiv preprint arXiv:2409.12191*, 2024.

Wang, S. and Kanwar, P. Bfloat16: The secret to high performance on cloud tpus. *Google Cloud Blog*, 4, 2019.

watsonx.data. Ibm watsonx.data. <https://www.ibm.com/products/watsonx-data>.

Wolf, T., Debut, L., Sanh, V., Chaumond, J., Delangue, C., Moi, A., Cistac, P., Rault, T., Louf, R., Funtowicz, M., and Brew, J. Huggingface’s transformers: State-of-the-art natural language processing. *ArXiv*, abs/1910.03771, 2019. URL <https://api.semanticscholar.org/CorpusID:208117506>.

Wolf, T., Debut, L., Sanh, V., Chaumond, J., Delangue, C., Moi, A., Cistac, P., Rault, T., Louf, R., Funtowicz, M., Davison, J., Shleifer, S., von Platen, P., Ma, C., Jernite, Y., Plu, J., Xu, C., Le Scao, T., Gugger, S., Drame, M., Lhoest, Q., and Rush, A. Transformers: State-of-the-art natural language processing. In Liu, Q. and Schlangen, D. (eds.), *Proceedings of the 2020 Conference on Empirical Methods in Natural Language Processing: System Demonstrations*, pp. 38–45, Online, October 2020. Association for Computational Linguistics. doi: 10.18653/v1/2020.emnlp-demos.6. URL <https://aclanthology.org/2020.emnlp-demos.6>.

Workshop, B., Scao, T. L., Fan, A., Akiki, C., Pavlick, E., Ilić, S., Hesslow, D., Castagné, R., Luccioni, A. S., Yvon, F., et al. Bloom: A 176b-parameter open-access multilingual language model. *arXiv preprint arXiv:2211.05100*, 2022.

Wortsman, M., Ilharco, G., Gadre, S. Y., Roelofs, R., Gontijo-Lopes, R., Morcos, A. S., Namkoong, H., Farhadi, A., Carmon, Y., Kornblith, S., and Schmidt, L. Model soups: averaging weights of multiple fine-tuned models improves accuracy without increasing inference time. 2022.

Wu, P. Pytorch 2.0: The journey to bringing compiler technologies to the core of pytorch (keynote). In *Proceedings of the 21st ACM/IEEE International Symposium on Code Generation and Optimization*, pp. 1–1, 2023.

Xiao, S., Liu, Z., Zhang, P., and Muennighoff, N. C-pack: Packaged resources to advance general chinese embedding, 2023.

Yadav, P., Tam, D., Choshen, L., Raffel, C., and Bansal, M. Ties-merging: Resolving interference when merging models. In *Thirty-seventh Conference on Neural Information Processing Systems*, 2023.

Yu Koh, J. Model zoo (hub), 2018. URL <https://modelzoo.co/>.

Zhang, C., Xie, Y., Bai, H., Yu, B., Li, W., and Gao, Y. A survey on federated learning. *Knowledge-Based Systems*, 216:106775, 2021.

Zhang, Q., Chen, M., Bukharin, A., He, P., Cheng, Y., Chen, W., and Zhao, T. Adaptive budget allocation for parameter-efficient fine-tuning. *arXiv preprint arXiv:2303.10512*, 2023.

Zhao, J., Zhang, Z., Chen, B., Wang, Z., Anandkumar, A., and Tian, Y. Galore: Memory-efficient llm training by gradient low-rank projection. *arXiv preprint arXiv:2403.03507*, 2024.

Zhao, Y., Gu, A., Varma, R., Luo, L., Huang, C.-C., Xu, M., Wright, L., Shojanazeri, H., Ott, M., Shleifer, S., et al. Pytorch fsdp: experiences on scaling fully sharded data parallel. *arXiv preprint arXiv:2304.11277*, 2023.

Zhu, M. and Gupta, S. To prune, or not to prune: exploring the efficacy of pruning for model compression. *arXiv preprint arXiv:1710.01878*, 2017.

ZipNN. Zipnn: A lossless compression library for ai pipelines, 2024. URL <https://github.com/zipnn/zipnn>.

Ziv, J. and Lempel, A. A universal algorithm for sequential data compression. *IEEE Transactions on Information Theory*, 23(3):337–343, 1977.

Ziv, J. and Lempel, A. Compression of Individual Sequences via Variable-Rate Coding. *IEEE Transactions on Information Theory*, 24(5):530–536, September 1978.

Álvaro Bartolomé Del Canto, Blázquez, G. M., Lajarín, A. P., and Suero, D. V. Distilabel: An ai feedback (aif) framework for building datasets with and for llms. <https://github.com/argilla-io/distilabel>, 2024.

.1 Models name Downloaded from Hugging Face

We provide a full list of the exact model names used as they appear in Hugging Face hub for complete reproducibility.

.1.1 Table 1

- BAAI/bge-base-en-v1.5 (Xiao et al., 2023)
- sentence-transformers/all-mpnet-base-v2 (Song et al., 2020)
- google-bert/bert-base-uncased (Devlin et al., 2019)
- Qwen/Qwen2.5-1.5B-Instruct (Team, 2024)
- openai/whisper-large-v2 (Radford et al., 2022)
- FacebookAI/xlm-roberta-large (Conneau et al., 2019)
- openai/clip-vit-base-patch32 (Radford et al., 2021)
- meta-llama/Llama-3.1-405B (Dubey et al., 2024)
- FacebookAI/roberta-base (Liu et al., 2019a)

.1.2 Table 2

- [jonatasgrosman/wav2vec2-large-xlsr-53-english](#) ([Baevski et al., 2020](#))
- [google-bert/bert-base-uncased](#) ([Devlin et al., 2019](#))
- [allenai/OLMo-1B-0724-hf](#) ([Groeneveld et al., 2024](#))
- [becausecurious/stable-video-diffusion-img2vid-fp16](#) ([Blattmann et al., 2023](#))
- [argilla/CapybaraHermes-2.5-Mistral-7B](#) ([Álvaro Bar-tolomé Del Canto et al., 2024](#))
- [FacebookAI/xlm-roberta-base](#) ([Conneau et al., 2019](#))
- [openai/clip-vit-large-patch14](#) ([Radford et al., 2021](#))
- [google-t5/t5-base](#) ([Raffel et al., 2020](#))
- [TheBloke/Llama-2-13B-Chat-fp16](#) ([Touvron et al., 2023](#))
- [TheBloke/tulu-7B-fp16](#) ([Ivison et al., 2023](#))
- [tiiuae/falcon-7b](#) ([Almazrouei et al., 2023](#))
- [bigscience/bloom](#) ([Workshop et al., 2022](#))
- [OpenBuddy/openbuddy-openllama-3b-v10-bf16](#) ([Geng & Liu, 2023](#))
- [mistralai/Mistral-7B-v0.1](#) ([Jiang et al., 2023](#))
- [meta-llama/Llama-3.1-8B-Instruct](#) ([Dubey et al., 2024](#))

.1.3 Figure 2

- [Qwen/Qwen2-VL-7B-Instruct](#) ([Wang et al., 2024](#))
- [meta-llama/Llama-3.1-8B-Instruct](#) ([Dubey et al., 2024](#))
- [ibm-granite/granite-7b-instruct](#) ([Granite Team, 2024](#))
- [microsoft/resnet-50](#) ([He et al., 2016](#))

.1.4 Figure 4

- [meta-llama/Llama-3.1-8B-Instruct](#) ([Dubey et al., 2024](#))
- [ibm-granite/granite-7b-instruct](#) ([Granite Team, 2024](#))
- [allenai/OLMo-1B-0724-hf](#) ([Groeneveld et al., 2024](#))

.1.5 Figure 6

- [FacebookAI/xlm-roberta-base](#) ([Conneau et al., 2019](#))

.1.6 Figure 7

- [FacebookAI/roberta-base](#) ([Liu et al., 2019b](#))

.1.7 Figure 9 + Table 3 + Figure 10

- [LLM360/Amber](#) ([Liu et al., 2023](#))
- [allenai/OLMo-1B-0724-hf](#) ([Groeneveld et al., 2024](#))
- [FacebookAI/xlm-roberta-large](#) ([Conneau et al., 2019](#))
- [meta-llama/Llama-3.1-8B-Instruct](#) ([Dubey et al., 2024](#))